Inorg. Chem. **2008**, *47*, 1663−1673

Structural and NMR Spectroscopic Investigations of Chair and Twist Conformers of the $P_2Se_8^{2-}$ Anion

Christiane Rotter, Michael Schuster, Mustafa Kidik, Oliver Schön, Thomas M. Klapötke, and Konstantin Karaghiosoff*

Department of Chemistry and Biochemistry, Ludwig-Maximilian University of Munich, Butenandtstr. 5-13(D), D-81377 Munich, Germany

Received August 3, 2007

Four new salts of the $P_2Se_8^{2-}$ anion have been prepared, starting from easily available reagents using different reaction strategies including reaction of the elements, oxidation of P_4Se_3 with alkalimetal diselenides and elemental selenium, and the use of an ionic liquid as a reaction medium. Multinuclear NMR investigations show the presence of both *chair*-$P_2Se_8^{2-}$ and *twist*-$P_2Se_8^{2-}$ in solution, with *twist*-$P_2Se_8^{2-}$ being the predominant conformer. The interconversion between the two conformers is slow on the NMR time scale. Structural investigations of the new salts by single-crystal X-ray diffraction show that *chair*-$P_2Se_8^{2-}$ is the conformer mostly found in the solid state. A first structural characterization of *twist*-$P_2Se_8^{2-}$ is reported. The bonding situation in the $P_2Se_8^{2-}$ anion as well as the relative stability of the chair, twist, and boat conformers was elucidated by quantum chemical calculations.

Introduction

In contrast to the well-known oxophosphates $P_nO_m^{x-}$, binary anions of phosphorus with the heavier chalcogens sulfur and selenium are less common and much less explored. Most of the contributions to the field of selenophosphates originate from the group of Kanatzidis and are limited to transition metal salts, which are insoluble in common organic solvents, thus making an investigation of their chemical properties difficult.[1] An important goal of our systematic investigations on the structures and chemical properties of phosphorus-rich and chalcogen-rich thio- and selenophosphate anions is the development of syntheses of soluble salts, which can be used for further reactions in solution.[2]

In the course of our investigations on chalcogenophosphates, our interest was attracted by the anion $P_2Se_8^{2-}$. This cyclic anion with a six-membered P−Se ring was first synthesized 1992 by Kolis et al.[3] The synthesis occurred via the reaction of P_4Se_4 glass with an excess of K_2Se_4 in DMF. The $P_2Se_8^{2-}$ anion was isolated as the $[Ph_4P]_2[P_2Se_8]$ salt with a yield of 36%. The compound was characterized using ^{31}P NMR spectroscopy and single-crystal X-ray diffraction. However, the synthesis of $P_2Se_8^{2-}$ by this route on a large scale is problematic because of the laborious preparation of the starting materials.

Here, we present the synthesis of new salts of the $P_2Se_8^{2-}$ anion starting from easily available materials and its characterization in solution by ^{31}P and ^{77}Se NMR spectroscopy as well as in the solid state by single-crystal X-ray diffraction.

Experimental Section

General. All reactions were carried out under an inert gas atmosphere using Schlenk techniques. Argon (Messer Griesheim, purity 4.6 in 50 l steel cylinder) was used as an inert gas. The used glass vessels were stored in a 130 °C drying oven. Before use, the glass vessels were flame-dried in a vacuum at 10^{-3} mbar.

P_4Se_3, the alkali metal selenides, and 1-butyl-3-methylimidazolium rhodanide were prepared as described in the literature and stored in a dry box under a nitrogen atmosphere.[4−6] Elemental selenium and lithium were used as received (Aldrich). The solvents

* Author to whom correspondence should be addressed. Phone: +49-89-2180-77426.Fax: +49-89-2180-77492. E-mail: klk@cup.uni-muenchen.de.

(1) (a) Kanatzidis, M. G. *Curr. Opin. Solid State Mater. Sci* **1997**, *2*, 139. (b) Chung, I.; Karst, A. L.; Weliky, D. P.; Kanatzidis, M. G. *Inorg. Chem.* **2006**, *45*, 2785. (c) Huang, S. P.; Kanatzidis, M. G. *Coord. Chem. Rev.* **1994**, *130*, 509.

(2) Schuster, M.; Karaghiosoff, K. *Phosphorus, Sulfur Silicon* **2001**, *168*, 117.

(3) Zhao, J.; Pennington, W. T.; Kolis, J. W. *J. Chem., Chem. Commun.* **1992**, 265.

(4) (a) Stoppioni, P.; Peruzzini, M. *Gazz. Chim. Ital.* **1988**, *118*, 581. (b) Schön, O. Ph.D. Thesis, LMU Munich, Munich, Germany, 2007..

(5) (a) Thompson, D. P.; Boudjouk, P. *J. Org. Chem.* **1988**, *53*, 2109. (b) Schuster, M. Ph.D. Thesis, LMU Munich, Munich, Germany, 1999..

(6) (a) Dyson, P. J.; Grossel, M. C.; Srinivasan, N.; Vine, T.; Welton, T.; Williams, D. J.; White, A. J. P.; Zigras, T. *J. Chem. Soc., Dalton Trans.* **1997**, 3465. (b) Kamal, A.; Chouhan, G. *Tetrahedron Lett.* **2005**, *46*, 1489.

10.1021/ic7015534 CCC: $40.75
Published on Web 02/01/2008

Table 1. Crystal and Structure Refinement Data

	$[Li(py)_4]_2[P_2Se_8]$ (**1**)	$[(nBu)_4N]_2[P_2Se_8]$•2 MeCN (**2**)	$[C_8H_{15}N_2]_2[P_2Se_8]$ (**3**)	$[Li(MeCN)_4]_2[P_2Se_8]$ (**4**)
empirical formula	$C_{20}H_{20}LiN_4PSe_4$	$C_{36}H_{78}N_4P_2Se_8$	$C_8H_{15}N_2P_{Se}4$	$C_{16}H_{24}Li_2N_8P_2Se_8$
formula mass	670.15	1260.67	486.03	1035.93
temp (K)	200	200	100	100
cryst size (mm)	0.2 × 0.1 × 0.05	0.3 × 0.3 × 0.2	0.25 × 0.2 × 0.15	0.3 × 0.2 × 0.2
cryst description	yellow rod	yellow rod	orange block	yellow rod
cryst syst	triclinic	monoclinic	monoclinic	orthorhombic
space group	$P\bar{1}$	$P2_1/c$	$P2_1/n$	*Pbam*
a (Å)	10.1582(8)	9.6284(5)	7.6642(10)	20.0535(6)
b (Å)	10.7716(8)	16.9553(8)	10.9948(2)	12.1200(5)
c (Å)	12.7499(10)	16.0899(7)	17.0380(3)	15.0831(6)
α (deg)	95.271(6)	90	90	90
β (deg)	94.847(6)	96.875(4)	91.211(2)	90
γ (deg)	114.219(7)	90	90	90
V (Å)	1255.40(17)	2607.8(2)	1435.41(4)	3665.9(2)
Z	2	2	4	4
ρ_{calcd} (g cm^{-1})	1.773	1.605	2.249	1.877
μ (mm^{-1})	5.922	5.694	10.308	8.081
F (000)	644	1248	912	1936
θ range (deg)	3.98–30.06	4.01–27.50	3.71–27.50	3.76–26.00
	$-14 \le h \le 14$	$-12 \le h \le 12$	$-9 \le h \le 9$	$-24 \le h \le 24$
	$-15 \le k \le 15$	$-22 \le k \le 22$	$-14 \le k \le 14$	$-14 \le k \le 14$
index ranges	$-17 \le l \le 17$	$-20 \le l \le 20$	$-22 \le l \le 22$	$-18 \le l \le 18$
reflns collected	17142	29439	15990	35613
reflcns observed	2885	4638	2547	3427
reflns unique	7312 (R_{iint} = 0.0792)	5975 (R_{iint} = 0.0730)	3287 (R_{iint} = 0.0337)	3732 (R_{iint} = 0.1607)
R1, wR2 (2σ data)	0.0481, 0.0534	0.0409, 0.0677	0.0281, 0.0715	0.1075, 0.1295
R1, wR2 (all data)	0.1739, 0.0802	0.0649, 0.0770	0.0425, 0.0763	0.1207, 0.1342
max/min transm	1.1604/0.7733	1.1938/0.7294	1.0000/0.7163	0.8572/0.4122
data/restr/params	7312/0/271	5975/0/227	3287/0/136	3732/0/190
GOF on F^2	0.897	1.060	1.160	1.364
larg. diff peak/hole (e/Å)	0.556/−0.439	0.616/−0.447	1.176/−0.658	1.535/−0.655

were dried using commonly known drying methods and were freshly distilled before use. Melting points were determined in capillaries using a Büchi B540 instrument and are uncorrected.

NMR Spectroscopy. NMR spectra were recorded using a Jeol EX 400 Eclipse instrument operating at 161.997 MHz (^{31}P), 76.321 MHz (^{77}Se), and 155.526 MHz (^{7}Li) and a Jeol GSX 270 Delta Eclipse instrument operating at 109.365 MHz (^{31}P) and 51.525 MHz (^{77}Se). Chemical shifts are referred to 85% H_3PO_4 (^{31}P), $(CH_3)_2Se$ (^{77}Se), and 0.1 M solution of LiCl in D_2O (^{7}Li) as external standards. All spectra were measured, if not mentioned otherwise, at 25 °C. For the simulation of the ^{31}P NMR spectra, the PERCH program package was used.[7]

X-ray Crystallography. The molecular structures in the crystalline state were determined using an Oxford Xcalibur3 diffraction instrument with a Spellman generator (voltage 50 kV, current 40 mA) and a Kappa CCD detector with an X-ray radiation wavelength of 0.71073 Å. The data collection was performed with the CrysAlis CCD software and the data reduction with the CrysAlis RED software.[8,9] The structures were solved with SIR-92, SIR-97, and SHELXS-97 and refined with SHELXL-97 and finally checked using PLATON.[10–14] The absorptions were corrected by a SCALE3 ABSPACK multiscan method.[15] All relevant data and parameters of the X-ray measurements and refinements are given in Table 1. Further information on the crystal structure determinations has been deposited with the Cambridge Crystallographic Data Centre as supplementary publication numbers 654159 (**2**), 654160 (**4**), 654161 (**1**), and 654162 (**3**).

$[Li(py)_4]_2[P_2Se_8]$ (1). P_4Se_3 (1.443 g, 4 mmol), lithium powder (111.1 mg, 16 mmol), and gray selenium (2.842 g, 36 mmol) in 8 mL of pyridine were stirred for 24 h. From the resulting yellow suspension, the solid was separated by filtration using a G4 frit. The yellow solution was stored at room temperature. After three days, yellow crystals of $[Li(py)_4]_2[P_2Se_8]$ were formed, which were separated by filtration and dried in vacuo. Yield: 2.9 g (90% with respect to P_4Se_3).

Alternatively, red phosphorus (62 mg, 2 mmol), lithium powder (14 mg, 2 mmol), and gray selenium (632 mg, 8 mmol) were heated in a glass flask for 24 h at 240 °C. After cooling to room temperature, the orange-red solid was dissolved in 10 mL of pyridine yielding an orange solution. The solution was stored at room temperature. After five days, yellow crystals of $[Li(py)_4]_2[P_2Se_8]$ were obtained. Yield: 1.89 g (71% with respect to P_4Se_3).

m.p.: 109 °C. ^{31}P{^{1}H} NMR (pyridine): δ −89.8 (*chair*-$P_2Se_8^{2-}$, 21%), −4.5 (*twist*-$P_2Se_8^{2-}$, 79%) ppm. ^{77}Se{^{1}H} NMR (pyridine): δ 241.8 (Se_{exo}, *chair*-$P_2Se_8^{2-}$, $^{1}J_{SeP}$ = 604 Hz), 390.0 (Se_{exo}, *chair*-$P_2Se_8^{2-}$, $^{1}J_{SeP}$ = 733 Hz), 453.7 (Se_{exo}, *twist*-$P_2Se_8^{2-}$, $^{1}J_{SeP}$ = 659 Hz), 762.2 (Se_{endo}, *twist*-$P_2Se_8^{2-}$, $^{1}J_{SeP}$ = 372 Hz, $^{2}J_{SeP}$ = 33 Hz), 910.0 (Se_{endo}, *chair*-$P_2Se_8^{2-}$, $^{1}J_{SeP}$ = 348 Hz) ppm. ^{7}Li{^{1}H} NMR (pyridine): δ 5.5 ppm.

(7) Laatikainen, R.; Niemitz, M.; Weber, U.; Sundelin, T.; Hasinen, T.; Vepsäläinen, J. *J. Magn. Reson. A* **1996**, *120*, 1.

(8) *CrysAlis CCD*, version 1.171.27p5 beta (release 01–04–2005 CrysAlis171.NET; compiled Apr 1 2005,17:53:34); Oxford Diffraction Ltd.: Oxfordshire, U.K.

(9) *CrysAlis RED*, version 1.171.27p5 beta (release 01–04–2005 CrysAlis171.NET; compiled Apr 1 2005, 17:53:34); Oxford Diffraction Ltd.: Oxfordshire, U.K.

(10) SIR-92, A Program for Crystal Structure Solution: Altomare, A.; Cascarano, G. L.; Giacovazzo, C.; Guagliardi, A. *J. Appl. Crystallogr.* **1993**, *26*, 343.

(11) Altomare, A.; Burla, M. C.; Camalli, M.; Cascarano, G. L.; Giacovazzo, C.; Guagliardi, A.; Moliterni, A. G. G.; Polidori, G.; Spagna, R. *J. Appl. Crystallogr.* **1999**, *32*, 115.

(12) Sheldrick, G. M. *SHELXS-97, Program for Crystal Structure Solution*; Universität Göttingen: Göttingen, Germany, 1997.

(13) Sheldrick, G. M. *SHELXL-97, Program for the Refinement of Crystal Structures*; University of Göttingen: Göttingen, Germany, 1997.

(14) Spek, L. A. *PLATON, A Multipurpose Crystallographic Tool*; Utrecht University: Utrecht, The Netherlands, 1999.

(15) *SCALE3 ABSPACK - An Oxford Diffraction program* (1.0.4, gui:1.0.3); Oxford Diffraction Ltd.: Oxfordshire, U.K., 2005.

$[n\mathrm{Bu_4N}]_2[P_2Se_8]\cdot 2$MeCN (2). P_4Se_3 (1.303 g, 3.6 mmol), Li_2Se_2 (1.293 g, 7.2 mmol), and gray selenium (2.567 g, 32.5 mmol) in 40 mL of acetonitrile were stirred at room temperature. After three days, a red reaction solution and small amounts of a dark solid (probably unreacted elemental selenium) were obtained. The dark solid was removed using a G4 frit. A solution of $n\mathrm{Bu_4NBr}$ (4.6 g, 14.3 mmol) in 20 mL of acetonitrile was added to the filtrate, and the resulting mixture was stored at room temperature. Within 24 h, yellow crystals of $[n\mathrm{Bu_4N}]_2[P_2Se_8]\cdot 2$MeCN formed, which were separated using a G3 frit, washed with 3×5 mL of cold acetonitrile and dried under vacuum. Yield: 5 g (91%, with respect to P_4Se_3).

Alternatively, P_4 (1.92 g, 15.5 mmol), Li_2Se_2 (5.32 g, 31.0 mmol), and gray selenium (14.48 g, 186 mmol) in 60 mL of acetonitrile were stirred at room temperature. After five days, a red-brown solution over a dark gray solid (probably unreacted elemental selenium) was formed. The solid was removed by filtration using a G4 frit. Subsequently, a solution of $n\mathrm{Bu_4NBr}$ (19.65 g, 60.95 mmol) in 40 mL of acetonitrile was added to the yellow filtrate, and the reaction mixture was stored at room temperature. Within one day, yellow crystals of $[n\mathrm{Bu_4N}]_2[P_2Se_8]\cdot 2$MeCN were formed, which were separated via a G3 frit, washed with 2×3 mL of cold acetonitrile and dried under vacuum. Yield: 22.3 g (87% with respect to P_4Se_3).

m.p.: 99−101 °C. $^{31}P\{^1H\}$ NMR (CH_3CN): δ −4.5 (*twist*-$P_2Se_8^{2-}$, 78%), −89.8 (*chair*-$P_2Se_8^{2-}$, 22%) ppm. $^{77}Se\{^1H\}$ NMR (CH_3CN): δ 242.0 (Se_{exo}, *chair*-$P_2Se_8^{2-}$, $^1J_{SeP} = 604$ Hz), 390.0 (Se_{exo}, *chair*-$P_2Se_8^{2-}$, $^1J_{SeP} = 733$ Hz), 453.6 (Se_{exo}, *twist*-$P_2Se_8^{2-}$, $^1J_{SeP} = 659$ Hz), 762.2 (Se_{endo}, *twist*-$P_2Se_8^{2-}$, $^1J_{SeP} = 372$ Hz, $^2J_{SeP} = 33$ Hz), 910.3 (Se_{endo}, *chair*-$P_2Se_8^{2-}$, $^1J_{SeP} = 348$ Hz, $^2J_{SeP} = 33$ Hz) ppm. Anal. Calcd for $C_{36}H_{78}N_4P_2Se_8$: C, 34.79; H, 6.24; N, 4.44. Found: C, 34.83; H, 6.27; N 4.39.

$[\mathrm{bmim}]_2[P_2Se_8]$ (3). P_4Se_3 (360 mg, 1 mmol), Na_2Se_2 (815 mg, 4 mmol), and gray selenium (711 mg, 9 mmol) in 1-butyl-3-methylimidazolium thiocyanate were stirred for 12 h at room temperature. During this time, the reagents dissolved completely and an orange solution was obtained. From this solution, orange crystals of $[\mathrm{bmim}]_2[P_2Se_8]$ separated after one day, which were isolated by filtration, washed with 7 mL of cold CH_2Cl_2, and dried in vacuo. Yield: 261 mg (54% with respect to P_4Se_3), m.p.: 109−112 °C.

$[\mathrm{Li(MeCN)_4}]_2[P_2Se_8]$ (4). P_4Se_3 (1.443 g, 4 mmol), Li_2Se (742.7 mg, 8 mmol), and gray selenium (2.21 g, 28 mmol) in 8 mL of acetonitrile were stirred at room temperature for a period of 12 h. The red-brown suspension was filtrated using a G4 frit, and to the orange clear filtrate was added a spatula-point of CuCl. The solution turned red and was stored in the fridge at +4 °C. After one day, $[\mathrm{Li(MeCN)_4}]_2[P_2Se_8]$ separated as yellow crystals. Yield: 1.21 g (58% with respect to P_4Se_3). m.p.: 14–16 °C. $^{31}P\{^1H\}$ NMR (MeCN): δ −4.5 (*twist,* 58%), −89.8 (*chair*, 14%) ppm.

Results and Discussion

Syntheses. The $P_2Se_8^{2-}$ anion is readily obtained by the oxidation of white phosphorus with an alkali metal diselenide M_2Se_2 (M = Li, Na) and gray selenium in the appropriate stoichiometric ratio using basic solvents like *N*-methyl imidazole, N,N′-dimethylpropyleneurea, or pyridine. Alternatively, P_4Se_3 can be used instead of P_4 in the reaction with M_2Se_2 and gray selenium (Scheme 1).

The reactions can be performed on a large scale and yield $P_2Se_8^{2-}$ as the predominating phosphorus-containing species in solution. The use of Li_2Se_2 has the advantage that common organic solvents like MeCN or THF can also be employed.

Scheme 1. Syntheses of New Salts with the $P_2Se_8^{2-}$ Anion

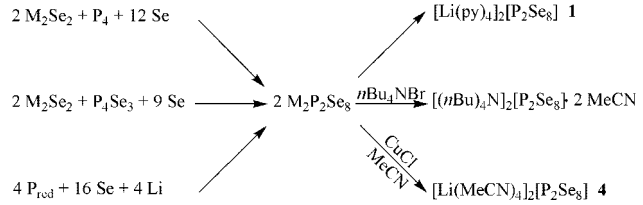

Scheme 2. Synthesis of $[\mathrm{bmim}]_2[P_2Se_8]$ in Ionic Liquid

$$P_4Se_3 + 2Na_2Se_2 + 9Se \xrightarrow{[\mathrm{bmim}]SCN} 2[\mathrm{bmim}]_2[P_2Se_8]\ (\mathbf{3})$$

Scheme 3. Twist, Chair, and Boat Conformers of the P_2Se_8 Dianion

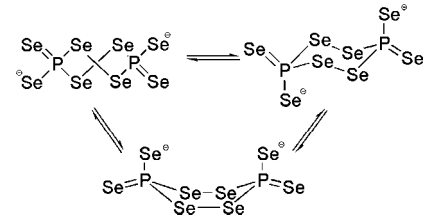

Exchange of the alkali metal cation by $n\mathrm{Bu_4N^+}$ in acetonitrile yields $[n\mathrm{Bu_4N}]_2[P_2Se_8]\cdot 2$MeCN (**2**) as yellow crystals in gram quantities.

Lithium salts of the $P_2Se_8^{2-}$ anion can be readily obtained by reaction of the elements. Heating of red phosphorus together with the stoichiometric amount of lithium and elemental selenium at 240 °C for 24 h results in the formation of an orange-red solid, which readily dissolves in pyridine or acetonitrile. From these solutions, yellow crystals of the lithium salts $[\mathrm{Li(py)_4}]_2[P_2Se_8]$ (**1**) and $[\mathrm{Li(MeCN)_4}]_2[P_2Se_8]$ (**4**) are formed. In the second case, crystallization occurred only after the addition of a small amount of CuCl and yielded a first example of a salt with the $P_2Se_8^{2-}$ anion in the twist conformation.

Ionic liquids like [bmim]SCN (bmim = 1-butyl-3-methylimidazolium cation) can also be used as a reaction medium of high polarity, which favors the formation of selenophosphate anions. When Na_2Se_2 is reacted with P_4Se_3 and elemental selenium in [bmim]SCN (Scheme 2), orange crystals of the new selenophosphate salt $[\mathrm{bmim}]_2[P_2Se_8]$ (**3**) are isolated in high yield. In this case, the cation of the salt is provided by the ionic liquid.

The isolated new salts of the $P_2Se_8^{2-}$ anion are moderately sensitive toward air and moisture and should be stored under an inert atmosphere. They are readily soluble in common organic solvents like acetonitrile, benzonitrile, propionitrile, and pyridine.

Multinuclear NMR Spectroscopy of the $P_2Se_8^{2-}$ Anion. There are three possible conformations for the six-membered ring in $P_2Se_8^{2-}$: chair, boat, and twist conformations (Scheme 3). In contrast to what has been reported in the literature, we observe in solutions of $P_2Se_8^{2-}$ always two ^{31}P NMR signals at −4.5 and −89.8 ppm, which are attributed to the twist and the chair conformers, respectively.[3] The ratio between the twist and the chair conformers is 4:1 in all of the solvents investigated. A ^{31}P NMR signal, indicating the presence of a boat conformer, was not observed.

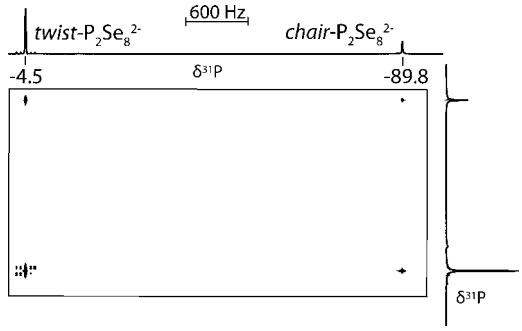

Figure 1. $^{31}P,^{31}P$ EXSY spectrum of $P_2Se_8^{2-}$ in acetonitrile (0.16 M, matrix 2048 × 1024, mixing time 0.5 s).

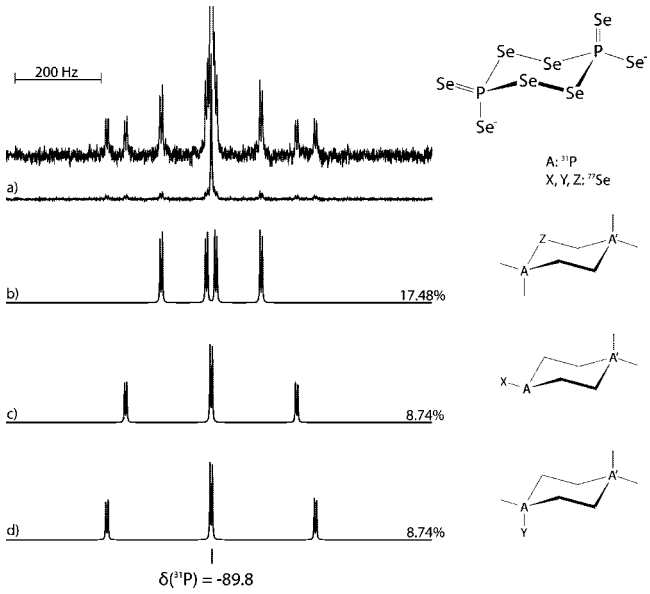

Figure 2. $^{31}P\{^1H\}$ NMR spectrum of *chair*-$P_2Se_8^{2-}$: (a) observed spectrum at –20 °C in acetonitrile (0.16 M, 1200 scans with a PD = 0.5 s, 30 min measuring time, υ_0 = 109.365 MHz, broadband ^1H decoupling, 0.5 Hz line broadening, satellite signals enhanced), (b−d) calculated spectra for the isotopomers with one ^{77}Se nucleus.

Interconversion between the conformers at ambient temperature is slow on the NMR time scale. The presence of a dynamic equilibrium between the twist and the chair conformers is clearly indicated by a $^{31}P,^{31}P$ exchange spectroscopy (EXSY) NMR spectrum (Figure 1), which shows cross peaks between the signals of the two conformers.

^{31}P NMR Spectra of *chair*-$P_2Se_8^{2-}$. The ^{31}P NMR signal for the chair conformer of the $P_2Se_8^{2-}$ anion in acetonitrile was observed at –89.8 ppm (Figure 2). The signal pattern consists of a singlet and three pairs of ^{77}Se satellites. The observed pattern is in accord with the C_{2h} symmetry of *chair*-$P_2Se_8^{2-}$, which implies the presence of two different exocyclic selenium nuclei. The singlet is caused by the isotopomer without ^{77}Se nuclei in the anion. The three pairs of ^{77}Se satellites display an intensity ratio of 2:1:1 and originate from isotopomers with one ^{77}Se nucleus. They all show the typical pattern of the A part of AA′X spectra with $^3J_{AA'} = {}^3J_{PP}$ of 8 Hz. The pair of satellites with the highest intensity is due to the isotopomer with one endocyclic ^{77}Se nucleus ($^1J_{SeP}$ = 348 Hz, $^2J_{SeP}$ = 33 Hz), while the other two pairs of satellites of equal intensity are caused by the isotopomers with a ^{77}Se nucleus in the exocyclic position (axial or equatorial). The corresponding $^1J_{SeP}$ coupling constants are 604 and 733 Hz.

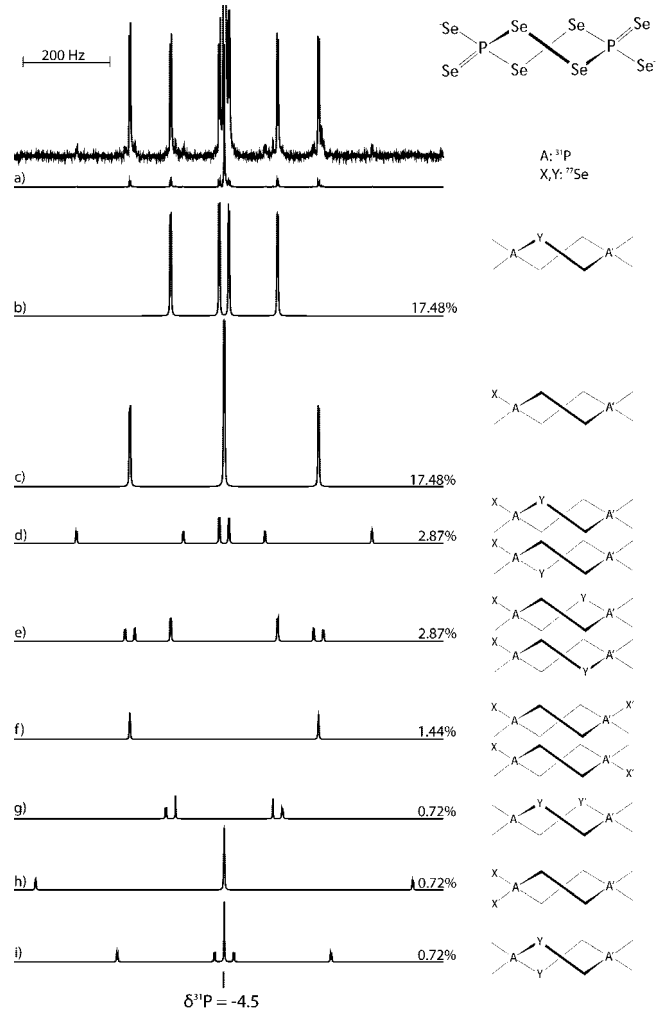

Figure 3. $^{31}P\{^1H\}$ NMR spectrum of *twist*-$P_2Se_8^{2-}$: (a) observed spectrum at –20 °C in acetonitrile (0.16 M, 1200 scans with a PD = 0.5 s, 30 min measuring time, υ_0 = 109.365 MHz, broadband ^1H decoupling, 0.5 Hz line broadening, satellite signals enhanced), (b and c) calculated spectra for the isotopomers with one ^{77}Se nucleus, (d−i) calculated spectra for the isotopomers with two ^{77}Se nuclei.

^{31}P NMR Spectra of *twist*-$P_2Se_8^{2-}$. For *twist*-$P_2Se_8^{2-}$, the ^{31}P NMR spectrum shows a singlet at −4.5 ppm, which is accompanied by two pairs of ^{77}Se satellites of equal intensity (Figure 3). The two pairs of satellites both display the line pattern typical for the A part of AA′X spectra and are caused by the isotopomers with one ^{77}Se nucleus in endocyclic ($^1J_{SeP}$ = 372 Hz) and exocyclic ($^1J_{SeP}$ = 659 Hz) position. The two exocyclic selenium nuclei are isochronous, which is in accord with the twist conformation of the anion. The P,P coupling constant $^3J_{PP} = {}^3J_{AA'}$ is 4 Hz smaller compared to that of *chair*-$P_2Se_8^{2-}$.

^{77}Se NMR Spectrum of *twist*- and *chair*-$P_2Se_8^{2-}$. In the ^{77}Se NMR spectrum (Figure 4), the signal for the endocyclic selenium atoms of the chair conformer appears at 910 ppm as a doublet of doublets ($^1J_{SeP}$ = 348 Hz). The observed four-line pattern (instead of the anticipated five lines for the X part of AA′X) results from the small P,P coupling constant, which implies only a small deviation from the first-order splitting. For the exocyclic selenium atoms, two doublets at

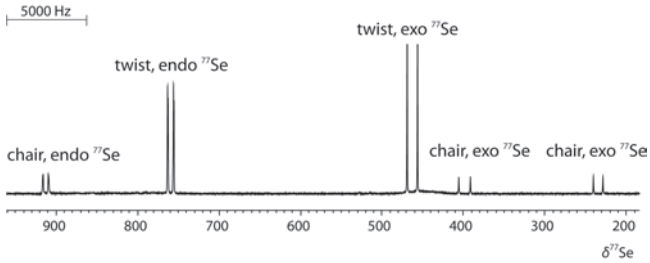

Figure 4. $^{77}Se\{^1H\}$ NMR spectrum of *twist*- and *chair*-$P_2Se_8^{2-}$: observed spectrum at 20 °C in *N*-methylimidazol (0.1 M, 92500 scans with a PD = 0.3 s, 19 h measuring time, v_0 = 51.525 MHz, broadband decoupling, 2 Hz line broadening).

390 ($^1J_{SeP}$ = 733 Hz) and 242 ppm ($^1J_{SeP}$ = 604 Hz) are observed. On the basis of the quantum chemical calculations (see below), they are assigned to the selenium atoms in axial and equatorial positions, respectively.

In the ^{77}Se NMR spectrum of the twist conformer, signals at 762 ppm ($^1J_{SeP}$ = 372 Hz, $^2J_{SeP}$ = 33 Hz) and at 454 ppm ($^1J_{SeP}$ = 659 Hz) are observed for the endocyclic and exocyclic selenium atoms, respectively.

Crystal and Molecular Structures of $P_2Se_8^{2-}$ Salts. The structure of the $P_2Se_8^{2-}$ anion in four different salts was determined using single-crystal X-ray diffraction. In the following section, the structures of the different salts are first discussed individually and are then compared with each other.

$[Li(py)_4]_2[P_2Se_8]$ (1). Block-shaped single crystals of $[Li(py)_4]_2[P_2Se_8]$ (**1**) suitable for X-ray diffraction were obtained by keeping a pyridine solution of the salt for several days at ambient temperature. The compound crystallizes in the triclinic space group $P\bar{1}$ with two formula units in the unit cell.

The $P_2Se_8^{2-}$ anion adopts a chair conformation with C_{2h} symmetry (Figure 5). The P−Se bond lengths to the exocyclic selenium atoms are 214.3(1) pm (P1−Se4) and 210.3(1) pm (P1−Se3) between the values for a P−Se single bond and those found for the P−Se bond in phosphine selenides.[16] The endocyclic P−Se distances correspond with 227.6(1) pm (P1−Se1) and 227.4(1) pm (P1(i)−Se2) to P−Se single bonds. The Se−Se bond length is 234.2(1) pm, which is in good agreement with the value expected for a Se−Se single bond.[17] The phosphorus atom is surrounded in a distorted tetrahedral arrangement by four selenium atoms. The endocyclic Se1−P1−Se2(i) angle is 104.4(1)°, whereas the exocyclic Se−P−Se angles range between 99° and 124°. Selected structural parameters for the $P_2Se_8^{2-}$ anion in compound **1** are given in Table 2. The angles at the endocyclic selenium atoms are 103.0(1)° and 102.0(1)°. For the torsion angles P1−Se1−Se2−P1(i) and Se2−Se1−P1−Se2(i), values of 71.9(1)° and 73.0(1)° are observed.

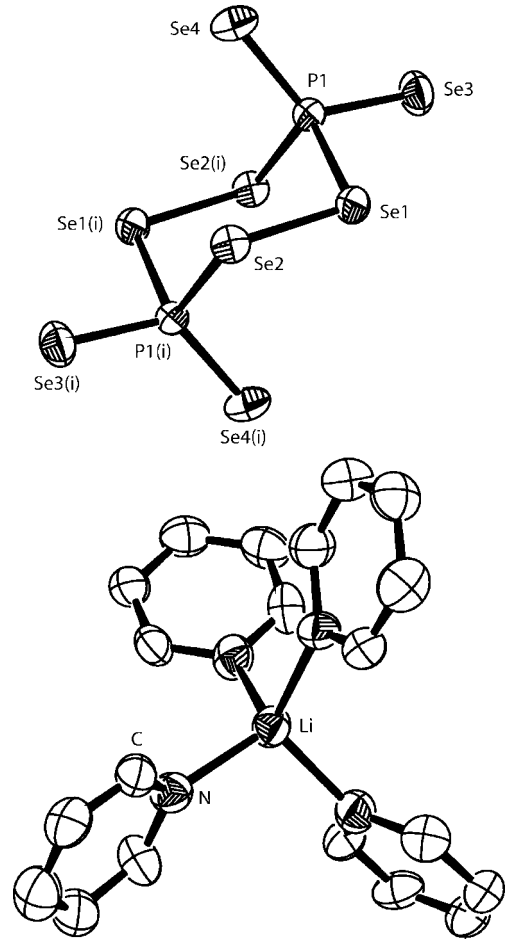

Figure 5. Molecular structure of one ion pair in $[Li(py)_4]_2[P_2Se_8]$ (**1**) in the crystal. Viewed along the *b* axis; ellipsoids are drawn at the 50% probability level; $i = 1 - x, 1 - y, -z$.

Table 2. Selected Bond Lengths (pm) and Angles (deg) of $[Li(py)_4]_2[P_2Se_8]$ (**1**)

bond lengths [pm]			
P1−Se1	227.6(1)	P1-Se3	214.3(1)
P1(i)−Se2	227.4(1)	Se1-Se2	234.2(1)
P1−Se4	210.3(1)		
bond angles [deg]			
Se1−P1−Se2(i)	104.4(1)	Se2(i)−P1−Se3	98.96(1)
Se2(i)−P1−Se4	113.69(1)	Se4−P1−Se1	113.2(1)
Se4−P1−Se3	124.2(1)	P1−Se1−Se2(i)	102.0(1)
Se3−P1−Se1	99.7(1)	P1(i)−Se2−Se1	103.0(1)
torsion angles [deg]			
P1−Se1−Se2−P1(i)	71.9(1)	Se2−Se1−P1−Se2(i)	−73.0(1)

$[n Bu_4N]_2[P_2Se_8]\cdot 2MeCN$ (2). Yellow block-shaped single crystals of $[nBu_4N]_2[P_2Se_8]\cdot 2MeCN$ (**2**) were obtained after the addition of tetra(*n*-butyl)ammonium bromide to a solution of $Na_2P_2Se_8$ in acetonitrile. Compound **2** crystallizes in the monoclinic space group $P2_1/c$ with four formula units in the unit cell.

The $P_2Se_8^{2-}$ anion lies on a crystallographic inversion center which is located in the middle of the chair-shaped $P_2Se_8^{2-}$ ring; therefore, half of the anion is generated by symmetry (Figure 6). The P−Se bond length between the phosphorus atom and the axial exocyclic Se atom (210.8(1)

(16) (a) Cordes, A. W. *Selenium*; Zingaro, R. A., Cooper, W. C., Eds.; Van Nostrand Reinhold Company: New York, 1974. (b) Shaw, R. A.; Woods, M.; Cameron, I. S.; Dahlen, B. *Chem. Ind.* **1971**, 151. (c) Grand, A.; Martin, J.; Robert, J. B.; Tordjman, I. *Acta Crystallogr., Sect. B* **1975**, *31*, 2523. (d) Galdecki, Z.; Glowka, M. L.; Michalski, J.; Okruszek, A.; Stec, W. J. *Acta Crystallogr., Sect. B* **1977**, *33*, 2322. (e) Cameron, T. S.; Howlett, K. D.; Miller, K. *Acta Crystallogr., Sect. B* **1978**, *34*, 1639. (f) Codding, P. W.; Kerr, K. A. *Acta Crystallogr., Sect. B* **1979**, *35*, 1261. (g) Romming, C.; Songstad, J. *Acta Chem. Scand.* **1979**, *A33*, 187.

(17) Holleman, A. F.; Wiberg, E.; Wiberg, N. *Lehrbuch der Anorganischen Chemie*, 101st ed.; Walter de Gruyter Verlag: Berlin, 1995.

Table 3. Selected Bond Lengths (pm) and Angles (deg) of $[(n\text{Bu})_4\text{N}]_2[\text{P}_2\text{Se}_8]\cdot 2\text{MeCN}$ (**2**)

	bond lengths [pm]		
P1−Se1	227.9(1)	P1−Se3	210.8(1)
P1(i)−Se2	228.0(1)	Se1−Se2	233.6(1)
P1−Se4	213.5(1)		
	bond angles [deg]		
Se1−P1−Se2(i)	103.3(1)	Se2(i)−P1−Se3	113.1(1)
Se4−P1−Se2(i)	101.4(1)	Se4−P1−Se1	100.0(1)
Se3−P1−Se4	123.1(1)	P1−Se1−Se2	102.4(1)
Se3−P1−Se1	113.4(1)	Se1−Se2−P1(i)	102.4(1)
	torsion angles [deg]		
P1−Se1−Se2−P1(i)	73.1(1)	Se2−Se1−P1−Se2(i)	−73.8(1)

Table 4. Selected Bond Lengths (pm) and Angles (deg) of $[\text{C}_8\text{H}_{15}\text{N}_2]_2[\text{P}_2\text{Se}_8]$ (**3**)

	bond lengths [pm]		
P1−Se1	227.7(1)	P1−Se3	210.7(1)
P1(i)−Se2	228.4(1)	Se1−Se2	234.4(1)
P1−Se4	213.1(1)		
	bond angles [deg]		
Se1−P1−Se2(i)	104.7(1)	Se2(i)−P1−Se3	112.9(1)
Se4−P1−Se2(i)	101.5(1)	Se4−P1−Se1	98.5(1)
Se3−P1−Se4	123.9(1)	P1−Se1−Se2(i)	103.7(1)
Se3−P1−Se1	112.9(1)	Se1−Se2−P1(i)	101.5(1)
	torsion angles [deg]		
P1−Se1−Se2−P1(i)	71.6(1)	Se2−Se1−P1−Se2(i)	−73.9(1)

Table 5. Selected Bond Lengths (pm) and Angles (deg) of $[\text{Li}(\text{MeCN})_4]_2[\text{P}_2\text{Se}_8]$ (**4**)

	bond lengths [pm]		
P1−Se1	228.0(1)	P1−Se3	212.9(1)
P1−Se2	228.9(1)	Se1−Se1(i)	232.4(1)
P1−Se4	212.5(1)	Se2−Se2(i)	232.3(1)
	bond angles [deg]		
Se1−P1−Se2	105.1(1)	Se2−P1−Se3	99.8(1)
Se4−P1−Se2	116.9(1)	Se4−P1−Se1	99.3(1)
Se3−P1−Se4	120.1(1)	P1−Se2−Se2(i)	102.5(1)
Se3−P1−Se1	115.5(1)	P1−Se1−Se1(i)	101.2(1)
	torsion angles [deg]		
P1−Se1−Se1(i)−P1(i)	88.4(1)	Se1(i)−Se1−P1−Se2	−40.7(1)
P1−Se2−Se2(i)−P1(i)	84.5(1)	Se2(i)−Se2−P1−Se1	−37.2(1)

pm) is shorter than that to the equatorial exocyclic selenium atom (213.5(1) pm). The P−Se distances to the endocyclic selenium atoms are, at 228.0(1) pm, for P1−Se1 and P1(i)−Se2 practically identical. The Se−Se distance within the diselenide moiety is 233.5(1) pm (Table 3). Bond lengths and angles of the $P_2Se_8^{2-}$ anion in compound **2** do not differ significantly from those observed in compound **1**. Again, the largest Se−P−Se angle at phosphorus (123.1(1)°) is that involving both exocyclic selenium atoms. The endocyclic angle Se1−P1−Se2(i) is, at 103.3(1)°, smaller. The P1−Se1−Se2 angle within the ring is 102.4(1)°. The two torsion angles are 73.1(1)° (P1−Se1−Se2−P1) and −73.8(1)° (Se2−Se1−P1−Se2).

Two seleniumphosphate anions are centered on the *bc* plane, while six other anions are located at the vertices of the unit cell (Figure 7). There are no other significant interactions in the structure than the electrostatic attraction between the cation and anion. It is worthwhile to mention the loose packing of the ions within the unit cell, and the presence of the acetonitrile solvent molecules in the space between the ions.

$[\text{bmim}]_2[\text{P}_2\text{Se}_8]$ (3). Orange block-shaped single crystals were isolated after one day from a solution containing P_4Se_3, Na_2Se_2, and gray selenium in 1-butyl-3-methyl-imidazoliumrhodanide [bmim][SCN]. Compound **3** crystallizes in the monoclinic space group $P2_1/n$ with four formula units in the unit cell.

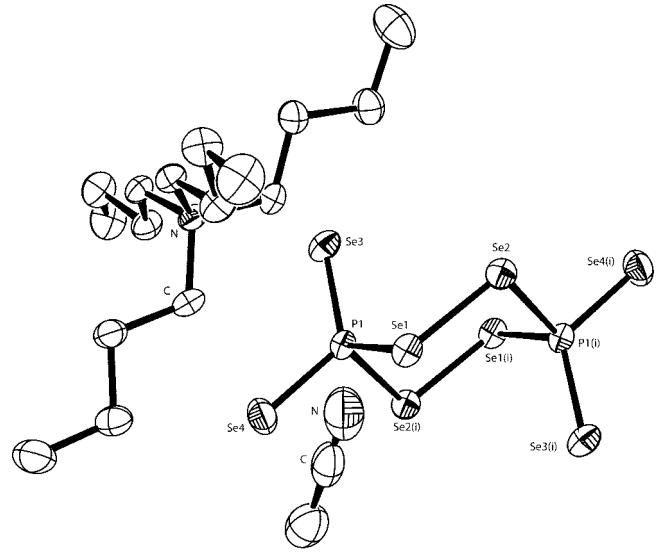

Figure 6. Molecular structure of $[(n\text{-Bu})_4\text{N}]_2[\text{P}_2\text{Se}_8]\cdot 2\text{MeCN}$ (**2**) in the crystal. Viewed along the *a* axis; ellipsoids are drawn at the 50% probability level; $i = 2 - x, 1 - y, 1 - z$.

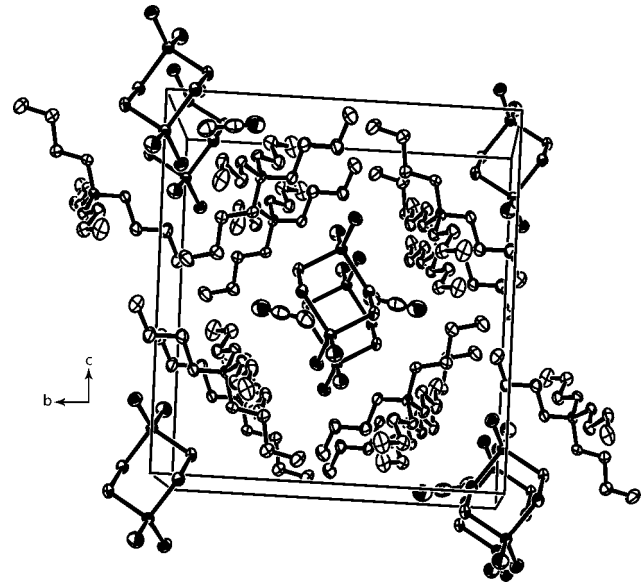

Figure 7. Crystal structure of $[(n\text{-Bu})_4\text{N}]_2[\text{P}_2\text{Se}_8]\cdot 2\text{MeCN}$ (**2**). View of the unit cell along the *a* axis; ellipsoids drawn at the 50% probability level.

The $P_2Se_8^{2-}$ anion adopts a chair conformation and is located on an inversion center; thus, half of the anion is generated by symmetry (Figure 8). The P−Se distances to the axial selenium atoms are, at 210.7(1) pm, slightly shorter than those to the equatorial exocyclic selenium atoms at 213.1(1) pm. The P−Se distances within the ring, Se1−P1 227.7(1) pm and Se2-P1(i) 228.4(1) pm, as well as the Se−Se distance of 234.4(1) pm fit well to those observed for the other $P_2Se_8^{2-}$ salts (Table 4).

The phosphorus atom is coordinated in a distorted tetrahedral arrangement by four selenium atoms with the largest Se−P−Se angle (123.9(1)°) involving the exocyclic

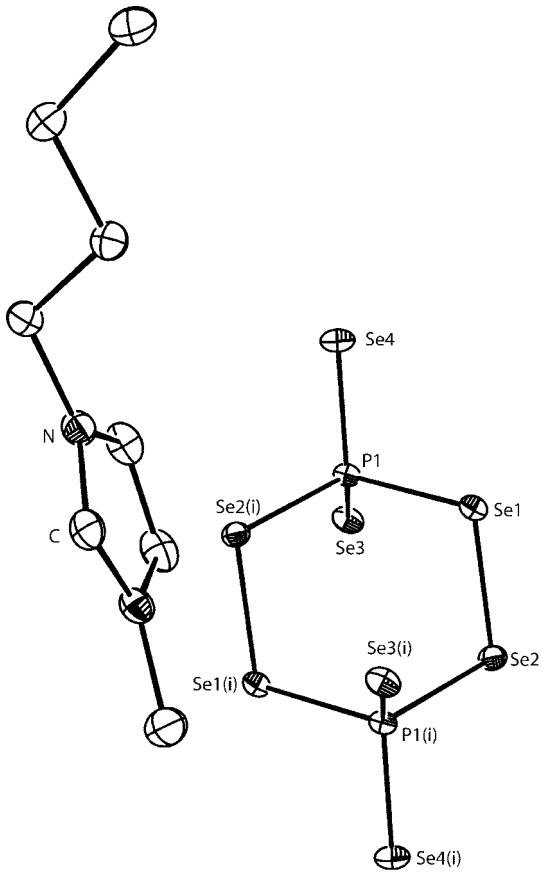

Figure 8. Molecular structure of $[C_8H_{15}N_2]_2[P_2Se_8]$ (**3**) in the crystal. View along the *c* axis; ellipsoids are drawn at the 50% probability level; $i = 1 - x, 1 - y, -z$.

selenium atoms. The Se2−Se1−P1 angle is 103.7(1)°, and the torsion angles adopt values of −73.9(1)° (Se2−Se1−P1−Se2(i)) and 71.6(1)° (P1−Se1−Se2−P1(i)).

In the crystal, the $P_2Se_8^{2-}$ anions lie on special positions within the unit cell (Figure 9). Two anions are located in the middle of the *ab* plane. Four other anions are placed on the edges of the unit cell along the *c* axis at a height of *c*/2. Anions and cations are arranged along the *a* axis. There are only electrostatic interactions between the cations and the anions.

$[Li(MeCN)_4]_2[P_2Se_8]$ (4): First Structure of *twist*-$P_2Se_8^{2-}$. In all of the crystal structures of $P_2Se_8^{2-}$ salts investigated so far, the anion was always found to adopt a chair conformation. In contrast, according to NMR spectroscopic investigations, the twist conformer predominates in solution. With $[Li(MeCN)_4]_2[P_2Se_8]$ (**4**), a first salt with the $P_2Se_8^{2-}$ anion adopting a twist conformation in the solid state was isolated and structurally characterized.

Yellow rod-shaped single crystals of compound **4** were obtained from an acetonitrile solution of $Li_2P_2Se_8$ after the addition of a small amount of CuCl at +4 °C. The crystals have a melting point around 15 °C. Compound **4** crystallizes in the orthorhombic space group *Pbam* with four formula units in the unit cell.

In the crystal, the $P_2Se_8^{2-}$ anion adopts twist conformation with D_2 symmetry and is located on a 2-fold axis of symmetry, which intercepts the Se−Se bond (Figure 10). Thus, half of the anion is generated by symmetry. The two P−Se distances to the exocyclic selenium atoms bonded to the same phosphorus atom are, at 212.5(1) pm (P1−Se4) and 212.9(1) pm (P1−Se3), very similar (Table 5). The observed values are closer to the distance generally found for phosphine selenides and are significantly smaller than a P−Se single-bond distance.[16,17] The endocyclic P−Se distances are, at 228.0(1) pm for P1−Se1 and 228.9(1) pm for P1−Se2, typical for P−Se single bonds.[17] The Se−Se distances within the diselenide units are, at 232.3(1) pm for Se2−Se2(i) and 232.4(1) pm for Se1−Se1(i), as expected.

The phosphorus atom displays a distorted tetrahedral coordination. The endocyclic angle at phosphorus is 105.1(1)°. As expected, the torsion angles within the ring (88.4(1)° for P1−Se1−Se1(i)−P1(i), 84.5(1)° for P1−Se2−Se2(i)−P1(i), −40.7(1)° for Se1(i)−Se1−P1−Se2, and −37.2(1)° for Se2(i)−Se2−P1−Se1) differ considerably from those observed in the structures of *chair*-$P_2Se_8^{2-}$.

In the crystal, cations and anions form stacks along the *c* axis (Figure 11). The unit cell of compound **4** comprises two complete $P_2Se_8^{2-}$ anions related by a mirror plane to each other, which is oriented orthogonal with respect to the *c* axis. Eight more $P_2Se_8^{2-}$ anions are located on the edges of the unit cell along the *c* axis. The lithium atoms are tetrahedrally coordinated, each by four acetonitrile molecules.

Comparison of the Structures of $P_2Se_8^{2-}$ Salts. For a comparison of the structural features of the $P_2Se_8^{2-}$ anion also, the only structurally characterized $P_2Se_8^{2-}$ salt described in the literature so far, $[Ph_4P]_2[P_2Se_8]$, is included.[3] The bond lengths and angles of the $P_2Se_8^{2-}$ anion in all of the salts structurally investigated do not differ significantly. Even in the twist conformation, there are no significant deviations of the bond lengths and angles as compared to those observed for the chair conformation. The P_2Se_4 six-membered ring of the $P_2Se_8^{2-}$ anion is remarkable, as to the best of our knowledge, there is only one example in the literature for a comparable six-membered ring with two diselenide units incorporated.[18] The Se−Se distances in this compound, *twist*-$(SiMe_2Ph)_4C_2Se_4$, are 231.2(1) and 230.9(1) pm and compare well with those found in the $P_2Se_8^{2-}$ salts.[18] The same applies also to the C−Se−Se−C torsion angles in *twist*-$(SiMe_2Ph)_4C_2Se_4$, which are with –78.7(2)° and −81.9(2)°, in the same range as those found for *twist*-$P_2Se_8^{2-}$ in compound **4**.

Computational Results. All calculations were carried out using the Gaussian G03W program code.[19] For the $[P_2Se_8]^{2-}$ anion, both the chair (**A**) and twist (**B**) conformers were observed experimentally by X-ray crystallography. In order to elucidate the structure, bonding, and energetics in the gas phase theoretically, computations were carried out using *ab initio* Hartree–Fock (HF) and hybrid density functional theory (DFT) at the B3LYP level (Becke's three-parameter hybrid functional, where the nonlocal correlation is provided by the LYP correlation functional, i.e. the correlation functional of Lee, Yang, and Parr).[20,21] Initially, the chair (**A**), twist (**B**), and boat (**C**) conformers were calculated without any

(18) Klapötke, T. M.; Krumm, B.; Polborn, K.; Scherr, M. *Eur. J. Inorg. Chem.* **2006**, 2937.

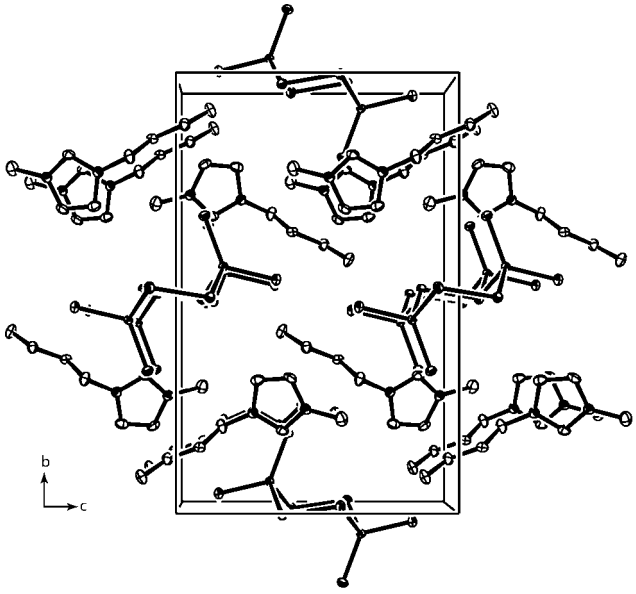

Figure 9. Crystal structure of $[C_8H_{15}N_2]_2[P_2Se_8]$ (**3**). View of the unit cell along the *a* axis; ellipsoids are drawn at the 50% probability level.

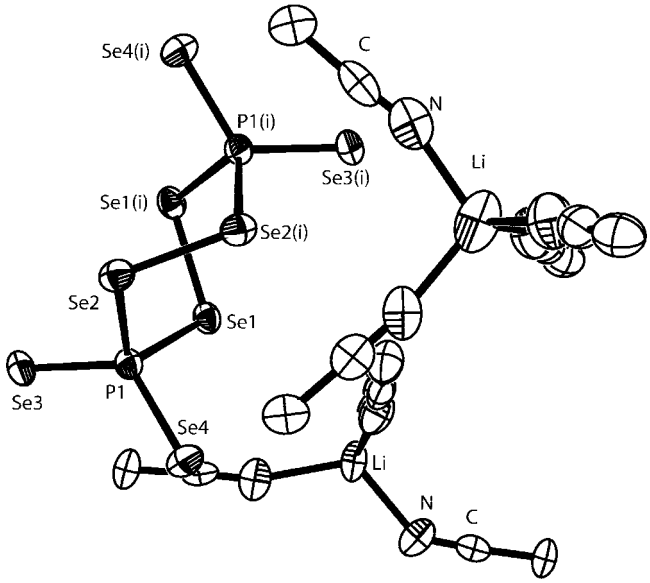

Figure 10. Molecular structure of $[Li(MeCN)_4]_2[P_2Se_8]$ (**4**) in the crystal. View along the *c* axis; ellipsoids are drawn at the 50% probability level, $i = -x, -y, -z$.

symmetry constraints employing an all-electron 3-21G(d) basis set.[22] At this level, the chair and twist conformers were found to be stable minima (NIMAG = 0) on the potential energy hypersurface, whereas the boat conformer was found to optimize to the chair structure. Consequently, all subsequent calculations were performed for the chair and twist conformers in C_{2h} and D_2 symmetry, respectively, at the HF and B3LYP levels of theory. Calculations employing a D95V basis for phosphorus and a quasirelativistic Stuttgart/Dresden pseudopotential (SDD) for the core electrons of selenium and a double-zeta basis for the valence electrons of Se resulted in optimized structures with overestimated (0.10–0.25 Å) bond lengths.

In order to obtain more reliable structural and thermochemical data, the chair and twist conformers of the $[P_2Se_8]^{2-}$ anion were then calculated at the B3LYP level of theory

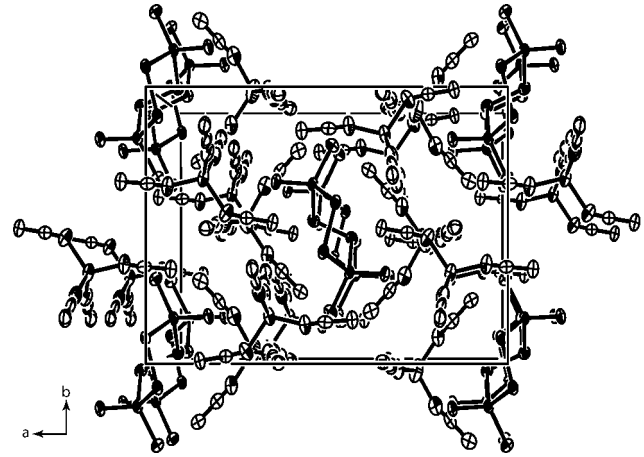

Figure 11. Crystal structure of $[Li(MeCN)_4]_2[P_2Se_8]$ (**4**). View of the unit cell all along the *c* axis; ellipsoids are drawn at the 50% probability level.

using an augmented polarized triple-zeta basis (6-311+G(d)) set for phosphorus and selenium (all-electron calculation).[24] The results are summarized in Table 6.

Both DFT calculations reproduce well the angles in the chair and twist conformers of the $[P_2Se_8]^{2-}$ dianion (Table 6). Whereas the SDD calculation always overestimated the Se−P and Se−Se bond lengths, the all-electron calculation

(19) Frisch, M. J.; Trucks, G. W.; Schlegel, H. B.; Scuseria, G. E.; Robb, M. A.; Cheeseman, J. R.; Montgomery, J. A., Jr.; Vreven, T.; Kudin, K. N.; Burant, J. C.; Millam, J. M.; Iyengar, S. S.; Tomasi, J.; Barone, V.; Mennucci, B.; Cossi, M.; Scalmani, G.; Rega, N.; Petersson, G. A.; Nakatsuji, H.; Hada, M.; Ehara, M.; Toyota, K.; Fukuda, R.; Hasegawa, J.; Ishida, M.; Nakajima, T.; Honda, Y.; Kitao, O.; Nakai, H.; Klene, M.; Li, X.; Knox, J. E.; Hratchian, H. P.; Cross, J. B.; Adamo, C.; Jaramillo, J.; Gomperts, R.; Stratmann, R. E.; Yazyev, O.; Austin, A. J.; Cammi, R.; Pomelli, C.; Ochterski, J. W.; Ayala, P. Y.; Morokuma, K.; Voth, G. A.; Salvador, P.; Dannenberg, J. J.; Zakrzewski, V. G.; Dapprich, S.; Daniels, A. D.; Strain, M. C.; Farkas, O.; Malick, D. K.; Rabuck, A. D.; Raghavachari, K.; Foresman, J. B.; Ortiz, J. V.; Cui, Q.; Baboul, A. G.; Clifford, S.; Cioslowski, J.; Stefanov, B. B.; Liu, G.; Liashenko, A.; Piskorz, P.; Komaromi, I.; Martin, R. L.; Fox, D. J.; Keith, T.; Al-Laham, M. A.; Peng, C. Y.; Nanayakkara, A.; Challacombe, P.; Gill, M. W.; Johnson, B.; Chen, W.; Wong, M. W.; Gonzalez, C.; and Pople, J. A.; *Gaussian 03*, Revision A.1; Gaussian, Inc.: Pittsburgh, PA, 2003.

(20) (a) Roothan, C. C. *J. Rev. Mod. Phys.* **1951**, *23*, 69. (b) Pople, J. A.; Nesbet, R. K. *J. Chem. Phys.* **1954**, *22*, 571. (c) McWeeny, R.; Dierksen, G. *J. Chem. Phys.* **1968**, *49*, 4852.

(21) (a) Lee, C.; Yang, W.; Parr, R. G. *Phys. Rev. B: Condens. Matter Mater. Phys.* **1988**, *37*, 785. (b) Miehlich, B.; Savin, A.; Stoll, H.; Preuss, H. *Chem. Phys. Lett.* **1989**, *157*, 200. (c) Becke, A. D. *J. Chem. Phys.* **1993**, *98*, 5648.

(22) (a) Binkley, J. S.; Pople, J. A.; Hehre, W. J. *J. Am. Chem. Soc.* **1980**, *102*, 939. (b) Gordon, M. S.; Binkley, J. S.; Pople, J. A.; Pietro, W. J.; Hehre, W. J. *J. Am. Chem. Soc.* **1982**, *104*, 2797. (c) Pietro, W. J.; Francl, M. M.; Hehre, W. J.; Defrees, D. J.; Pople, J. A.; Binkley, J. S. *J. Am. Chem. Soc.* **1982**, *104*, 5039. (d) Dobbs, K. D.; Here, W. J. *J. Comput. Chem.* **1986**, *7*, 359. (e) Dobbs, K. D.; Here, W. J. *J. Comput. Chem.* **1987**, *8*, 861. (f) Dobbs, K. D.; Here, W. J. *J. Comput. Chem.* **1987**, *8*, 880.

(23) (a) Dunning, T. H., Jr.; Hay, P. J. In *Modern Theoretical Chemistry*; Schaefer, H. F., III, Ed.; Plenum: New York, 1976. (b) Institut für Theoretische Chemie. http://www.theochem.uni-stuttgart.de/ (accessed Dec 2007).

(24) (a) McLean, A. D.; Chandler, G. S. *J. Chem. Phys.* **1980**, *72*, 5639. (b) Krishnan, R.; Binkley, J. S.; Seeger, R.; Pople, J. A. *J. Chem. Phys.* **1980**, *72*, 650. (c) Waters, A. J. H. *J. Chem. Phys.* **1970**, *52*, 1033. (d) Hay, P. J. *J. Chem. Phys.* **1977**, *66*, 4377. (e) Raghavachari, K.; Trucks, G. W. *J. Chem. Phys.* **1989**, *91*, 1062. (f) Binning, R. C., Jr.; Curtiss, L. A. *J. Comput. Chem.* **1990**, *11*, 1206. (g) Curtiss, L. A.; McGrath, M. P.; Blaudeau, J.-P.; Davis, N. E., Jr.; Radom, L. *J. Chem. Phys.* **1995**, *103*, 6104.

Table 6. Computational Results at the HF/6-311+G(d) and B3LYP/6-311+G(d) Levels of Theory for the *chair* (**A**) and *twist* (**B**) Conformers of $[P_2Se_8]^{2-}$

	chair-$[P_2Se_8]^{2-}$ (**A**)		*twist*-$[P_2Se_8]^{2-}$ (**B**)	
		HF/6-311+G(d)]		
symmetry	C_{2h}		D_2	
$-E$/au	19880.11168		19880.112539	
E_{rel}/kcal mol^{-1}	+ 0.9		0.0	
	calculated	experimental[a]	calculated	experimental
$d(Se_{term}-P)$/Å	2.15 (ax.), 2.17(eq.)	2.10 (ax.), 2.14 (eq.)	2.16	2.13
$d(Se_{ring}-P)$/Å	2.31	2.27	2.31	2.29
d(Se−Se)/Å	2.34	2.34	2.33	2.32
$<(Se_{term}-P-Se_{term})$/deg	120.7	124.2	119.0	120.2
$<(Se_{term}-P-Se_{ring})$/deg	113.9 (ax.), 102.1 (eq.)	113.7(ax,), 99.0 (eq.)	102.3, 114.5	99.3, 115.5
$<(P-Se_{ring}-Se_{ring})$/deg	104.9	103.0	102.9	102.6
		B3LYP/6-311+G(d)		
symmetry	C_{2h}		D_2	
$-E$/au	19895.465679		19895.469325	
E_{rel}/kcal mol^{-1}	+2.3		0.0	
	calculated	experimental	calculated	experimental
$d(Se_{term}-P)$/Å	2.14 (ax.), 2.18 (eq.)	2.10 (ax.), 2.14 (eq.)	2.17	2.13
$d(Se_{ring}-P)$/Å	2.37	2.27	2.37	2.29
d(Se−Se)/Å	2.37	2.34	2.36	2.32
$<(Se_{term}-P-Se_{term})$/deg	122.5	124.2	120.0	120.2
$<(Se_{term}-P-Se_{ring})$/deg	114.5 (ax.), 101.0 (eq.)	113.7, 99.0	100.4, 116.7	99.3, 115.5
$<(P-Se_{ring}-Se_{ring})$/deg	105.6	103.0	104.7	102.6

[a] Average values.

Table 7. Computed Isotropic Magnetic Shieldings (GIAO Method, HF/6-311+G(d))[19,26] and Relative ^{77}Se NMR Chemical Shifts (ppm) Referenced to Me_2Se

	abs. anisotropic shielding	rel. shift, δ/ppm	exptl. reported chem. shift, δ/ppm
Me_2Se	1946	0	0
MeSeH	2031	−85	−115[15]
$(CF_3)_2Se$	1308	638	717[15]
chair-$[P_2Se_8]^{2-}$	1160	786	ring 910
	1564	382	axial 390
	1689	262	equatorial 242
twist-$[P_2Se_8]^{2-}$	1252	694	ring 762
	1534	412	terminal 454

reproduces the experimentally observed structural parameters reasonably well (Table 6).

It also has to be stressed that all Se−Se and Se−P bond lengths were calculated for the isolated dianion in the gas phase where solid state effects are not taken into account. The fact that both calculations (SDD and all-electron) overestimated to some extent the bond lengths can be explained by the high negative charge concentration for an isolated (gas-phase) dianion, which is not necessarily the case for the condensed phase where significant cation-anion interactions result in a lowering of the negative charge on the dianion.

It is interesting to point out that the twist and chair conformers are *very* close in their total energies, with the twist conformer being thermodynamically more favorable (after zpe correction) by only 3.3 kcal mol^{-1} (B3LYP/SDD calculation) or 2.3 kcal mol^{-1} (B3LYP/6-311+G(d)):[25]

$$\textit{chair}\text{-}[P_2Se_8]^{2-} \rightarrow \textit{twist}\text{-}[P_2Se_8]^{2-} \qquad (1)$$

$$\Delta H(1) = -3.3 \text{ kcal/mol (B3LYP/SDD)}, -2.3 \text{ kcal/mol (B3LYP/6-311+G(d))}$$

(25) Klapötke, T. M.; Schulz, A.; Harcourt, R. D. *Quantum Chemical Methods in Main-Group Chemistry*; Wiley: Chichester, U.K., 1998.

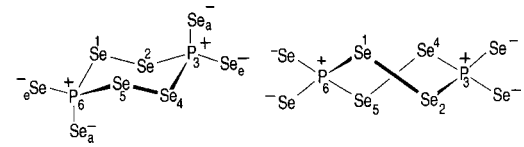

Figure 12. Natural Lewis structures for the *chair* (left) and *twist* (right) conformers of $[P_2Se_8]^{2-}$.

Table 8. NBO Natural Charges for the Chair (**A**) and Twist (**B**) Conformers of $[P_2Se_8]^{2-}$

	chair-$[P_2Se_8]^{2-}$ (**A**)	*twist*-$[P_2Se_8]^2$(**B**)
Se, terminal	axial: −0.62 equatorial: −0.68	−0.66
Se, ring	−0.10	−0.09
P	+ 0.50	0.50

The calculated similar relative energies of the twist and chair conformers are consistent with a recent combined theoretical and experimental study on the six-membered Se_4C_2 heterocycle *twist*-$(SiMe_2Ph)_4C_2Se_4$. [18] For this system, the twist conformer was calculated to be 1.9 kcal mol^{-1} more stable than the chair form.

With the reasonable assumption that $\Delta S(1) \approx 0$ (no significant change in entropy for the chair → twist conformation change; i.e., $\Delta G \approx \Delta H \approx$ 2.3–3.3 kcal mol^{-1}), the equilibrium constant for eq 1 can be estimated according to eq 2 to be 2.5–3.7. This indicates that solutions of the chair or twist conformer may often show detectable amounts of the other species present, with the twist concentration being 2.5–3.7 times higher than the concentration of the chair conformer. This is in good accord with the experimental value (see above), which suggests a 1:4 ratio.

$$K = -\exp\{\Delta G/RT\} \approx 2.5-3.7 \qquad (2)$$

The ^{77}Se NMR chemical shifts differ quite substantially for the chair and twist conformers of the $[P_2Se_8]^{2-}$ anion. In order to compute the NMR chemical shifts for both species, the isotropic magnetic shieldings were computed using the gauge-independent atomic orbital (GIAO) method imple-

Table 9. Computational Details for the Chair (**A**) and Twist (**B**) Conformers of $[P_2Se_8]^{2-}$

	chair-$[P_2Se_8]^{2-}$ (**A**)	*twist*-$[P_2Se_8]^{2-}$ (**B**)
symmetry	C_{2h}	D_2
$-E$/au	757.652644	757.657825
E_{rel}/kcal mol^{-1}	+3.3	0.0
NIMAG[a]	0	0
zpe[b]/kcal mol^{-1}	5.6	5.7
ν IR/Raman/cm^{-1}[c] (intensity)[d]		
d(Se$_{term}$−P) [X-ray]/Å	2.25 (ax.), 2.29 (eq.) [2.10 (ax.), 2.14 (eq.)]	2.27[2.13]
d(Se$_{ring}$−P) [X-ray]/Å	2.54 [2.27]	2.54 [2.29]
d(Se−Se) [X-ray]/Å	2.43 [2.34]	2.42 [2.32]
<(Se$_{term}$−P−Se$_{term}$) [X-ray]/deg	122.4 [124.2]	120.3 [120.2]
<(Se$_{term}$−P−Se$_{ring}$) [X-ray]/deg	114.5 (ax.), 101.8 (eq.) [113.7, 99.0]	101.8, 116.0 [99.3, 115.5]
<(P−Se$_{ring}$−Se$_{ring}$) [X-ray]/deg	107.2 [103.0]	106.7 [102.6]
ν_{as}(Se$_{ring}$−Se$_{ring}$)	234 (2/0)	238 (1/11)
ν_{sym}(Se$_{ring}$−Se$_{ring}$)	244 (0/9)	250 (0/3)
ν_{as}(Se$_{ring}$−P)	254 (0/38)	253 (1/14)
ν_{sym}(Se$_{ring}$−P)	282 (45/0)	288 (34/4)
δ_{as}(Se$_{terminal}$−P)	326 (237/0)	333 (270/6)
δ_{sym}(Se$_{terminal}$−P)	335 (0/17)	343 (0/12)
ν_{sym}(Se$_{terminal}$−P)	428 (168/0)	417 (162/16)
ν_{as}(Se$_{terminal}$−P)	429 (0/55)	421 (3/39)

[a] Number of imaginary frequencies. [b] Zero point energy. [c] Only vibrations with $\nu > 200$ cm^{-1} have been included into the table. [d] IR intensities in km mol^{-1}; Raman activities in Å^4 amu^{-1}.

mented in Gaussian03.[19,26] Since the DFT functionals do not include a magnetic field dependence, and therefore the DFT method does not provide systematically better NMR results than Hartree–Fock, the NMR shielding tensors were calculated at the HF/6-311+G(d) level of theory using the GIAO method.[26] Table 7 summarizes the computed isotropic magnetic shieldings, and relative ^{77}Se NMR chemical shifts (ppm) are referenced to Me_2Se. Table 7 also contains the experimentally reported and calculated chemical shifts of Me_2Se, MeSeH, and $(CF_3)_2Se$ to provide an assessment of the accuracy of the calculated values.

We also calculated the ^{31}P chemical shifts using the GIAO method at the same level of theory as for the ^{77}Se NMR shifts (HF/6-311+G(d)). The computed ^{31}P chemical shifts clearly predict a downfield shift of the twist conformer with respect to the chair conformer of 61 ppm, which is qualitatively in good agreement with the experimentally observed chemical shifts of $\delta = -89.8$ ppm (chair) and $\delta = -4.5$ ppm (twist) ($\Delta\delta = 85$ ppm).

For the chair and twist conformers of the $[P_2Se_8]^{2-}$ anion, a natural bond orbital (NBO) analysis was performed at the RHF/6-311+G(d) level of theory.[28] The most important natural Lewis structures (according to the NBO analysis) are shown in Figure 12. It is interesting to note that for the chair conformer the four most important (identical) intramolecular donor–acceptor interactions are of the following types:

π-LP(Se$_{axial}$) → σ^*(P3−Se2$_{ring}$)
π-LP(Se$_{axial}$) → σ^*(P3−Se4$_{ring}$)
π-LP(Se$_{axial}$) → σ^*(P6−Se1$_{ring}$)
π-LP(Se$_{axial}$) → σ^*(P6−Se5$_{ring}$)

with a donor–acceptor interaction energy of 15.1 kcal mol^{-1} each. The fact that the axial terminal Se atoms interact more strongly with the antibonding σ^*(P−Se$_{ring}$) bonds than the equatorial terminal Se atoms do is in good accord with the findings for six-membered organic ring compounds in the chair conformation (anomeric effect).[29] The computed NBO natural charges are summarized in Table 8, and computational details for the chair and twist conformations are given in Table 9.

For the twist conformer, there are again four energetically identical intramolecular donor–acceptor interactions:

π-LP(Se$_{terminal}$) → σ^*(P3−Se2$_{ring}$)
π-LP(Se$_{terminal}$) → σ^*(P3−Se4$_{ring}$)
π-LP(Se$_{terminal}$) → σ^*(P6−Se1$_{ring}$)
π-LP(Se$_{terminal}$) → σ^*(P6−Se5$_{ring}$)

In this case, all four terminal Se atoms donate lone-pair π electron density into the antibonding σ^*(P−Se$_{ring}$) bonds, which results in larger (116.0° and 116.7°; Table 6) Se$_{terminal}$−P−Se$_{ring}$ angles. The donor–acceptor interaction energies were all calculated to be 18.5 kcal mol^{-1} each. The computed NBO natural charges are also summarized in Table 8.

Conclusion

Starting from readily available reagents and following the synthetic routes described in this study, stable, and in common organic solvents, soluble salts of the selenophosphate anion $P_2Se_8^{2-}$ become available in preparatively useful quantities. The availability of $P_2Se_8^{2-}$ salts on a large scale opens the door to a systematic study of its coordination chemistry, which might lead to new transition metal selenophosphate-based materials prepared by "wet" synthesis under kinetically controlled conditions, and which is under current investigation in our laboratory. The synthetic strate-

(26) (a) Wolinski, K.; Hilton, J. F.; Pulay, P. *J. Am. Chem. Soc.* **1990**, *112*, 8251. (b) Dodds, J. L.; McWeeny, R.; Sadlej, A. J. *Mol. Phys.* **1980**, *41*, 1419. (c) Ditchfield, R. *Mol. Phys.* **1974**, *27*, 789. (d) McWeeny, R. *Phys. Rev.* **1962**, *126*, 1028.
(27) Klapötke, T. M.; Broschag, M. *Compilation of Reported 77Se NMR Chemical Shifts*; Wiley: Chichester, U.K., 1996.
(28) Weinhold, F. Natural Bond Orbital Methods. In *Encyclopedia of Computational Chemistry*; Schleyer, P. v. R, Ed.; Wiley: Chichester, U.K., 1998; Vol. 3 and references therein.
(29) Klapötke, T. M.; Schulz, A.; Harcourt, R. D. *Quantum Chemical Methods in Main- Group Chemistry*; Wiley: Chichester, U.K., 1998.

gies applied for the synthesis of the $P_2Se_8^{2-}$ salts, and in particular the use of ionic liquids, provide useful methods for the preparation of selenophosphates in general.

The X-ray crystallographic studies on $[Li(py)_4]_2[P_2Se_8]$, $[nBu_4N]_2[P_2Se_8]$·2MeCN, $[bmim]_2[P_2Se_8]$, and $[Li(MeCN)_4]_2[P_2Se_8]$ demonstrate the mobility of the system investigated. Small changes in the cation and in the crystallization conditions are sufficient to stabilize the chair conformer of $P_2Se_8^{2-}$ in the solid state, which is found in most cases, although the twist conformer predominates in solution. The results indicate only small energy differences between selenophosphate conformations, and this is supported by quantum chemical calculations.

Acknowledgment. Financial support by the Department of Chemistry and Biochemistry, University of Munich, is gratefully acknowledged. The authors thank also PD Dr. Margaret-Jane Crawford for many helpful discussions.

Supporting Information Available: Tables of atomic coordinates and crystallographic information (CIF) and further computational details. This material is available free of charge via the Internet at http://pubs.acs.org.

IC7015534